Assessing Effects of Near-Field Synergistic Light Absorption on Ordered Inorganic Phototropic Growth

Azhar I. Carim[†,§], Madeline C. Meier[†,§], Kathleen M. Kennedy[‡], Matthias H. Richter[‡], Kathryn R. Hamann[†] and Nathan S. Lewis[†,*]

[†]Division of Chemistry and Chemical Engineering, [‡]Division of Engineering and Applied Sciences, California Institute of Technology, Pasadena, California 91125, United States.

Supporting Information Placeholder

ABSTRACT: We report herein that synergistic light absorption in the optical near-field enables nanoscale self-organization during inorganic phototropic growth. Se-Te was grown electrochemically under illumination from an incoherent, unstructured light source in geometrically constrained, wavelength scale areas. Despite the limited dimensions, with as few as two discrete features produced in a single submicron dimension, the deposit morphology exhibited defined order and anisotropy. Computer modeling analysis of light absorption in simulated structures revealed a synergy wherein light capture in a nanoscale feature was enhanced by the presence of additional, adjacent features, with the synergistic effect originating predominantly from nearest neighbor contributions. Modeling moreover indicated that synergistic absorption is produced by scattering of the incident illumination by individual nanoscale features, leading to a local increase in the near-field intensity and consequently increasing the absorption in neighboring features. The interplay between these optical processes establishes the basis for spontaneous order generation via inorganic phototropic growth.

Most photosynthetic organisms exhibit phototropic growth, in which material grows to shape solar harvesting, and consequently display morphological phenotypes adapted to the light available in the habitat.[1-3] Chalcogen-based semiconductors exhibit analogous inorganic phototropic growth, in which highly ordered mesostructures formed in a bottom-up manner by photo-driven electrochemical deposition grow towards an incident light beam, and the resultant nanoscale feature dimensions, orientations and anisotropies are a function of the wavelength, polarization, incidence and phase characteristics of the optical excitation.[4-7] Inorganic phototropic growth occurs over macroscopic areas and utilizes unstructured, incoherent, and low-intensity illumination, an optically isotropic electrolyte, and no physical or chemical templating agents. In this work, we examine inorganic phototropic growth at physically confined, wavelength scale regions to understand short-range, cooperative optical communication amongst discrete nanoscale features in the near-field that yields the emergent and spontaneous self-organization of the resulting film morphology.

Figure 1a presents a representative scanning-electron micrograph (SEM) of a Se-Te deposit generated via inorganic phototropic growth on a planar, unpatterned, substrate. The deposit exhibited a highly anisotropic and ordered morphology consisting of vertically oriented lamellar features, in accord with prior work showing that on conductive, non-photoactive substrates (e.g. n^+-Si, Au) template-free growth of Se-Te, as well as Se-Pb and Se-Cd, can spontaneously generate periodic structures oriented along an arbitrarily selected incident optical polarization direction.[7-9] Here, inorganic phototropic growth was effected by light-mediated electrochemical synthesis of Se-Te from a solution of 0.0200 M SeO_2, 0.0100 M TeO_2, and 2.00 M H_2SO_4 using vertically polarized illumination with an intensity-weighted average wavelength (λ_{avg}) of 934 nm from an incoherent, narrowband light-emitting diode source. No photomask was used. The substrate was biased to enable the heterogenous electroreduction of the oxide precursors to the respective elemental states, effecting interfacial cathodic Se-Te deposition in accord with the following electrochemical half-reactions:

$$SeO_2 + 4H^+ + 4e^- \rightarrow Se + 4H_2O$$

$$TeO_2 + 4H^+ + 4e^- \rightarrow Te + 4H_2O$$

The applied bias is sufficient to drive film nucleation without the assistance of optical stimulation. The topology of this initial growth causes surficial scattering of the incident light beam which generates a spatially varying pattern of optical field intensity at the interface, with significant in-plane anisotropy when the stimulation is linearly polarized (see Supporting Information for additional details).[10] Local light absorption in an evolving Se-Te deposit accelerates the local rate of electroreduction and is

defined by the local field intenisty.[4] Thus, an anisotropic interfacial intensity pattern promotes anisotropic growth. This emergent film property focuses further anisotropic absorption and leads to the observed characteristics of inorganic phototropic growth.[5]

In-plane growth was then confined to dimensions that were comparable to the wavelength of the incident illumination by using substrates coated with a nonconductive poly(methyl methacrylate) (PMMA) layer in which circular well structures had been defined via electron-beam lithography. Growth proceeds via a light-stimulated electrochemical deposition process that cannot occur on regions of the substrate coated with an electrically insulating film such as PMMA. The well geometries did not limit mass transport between the bulk solution and the growth interface and did not influence the morphologies beyond the effect of lateral confinement. The concentration of precursor species is sufficiently large such that mass transport is not outpaced by the photo-driven electrochemical deposition. The circular geometry prevented the relative alignment of the optical polarization and the PMMA structures from affecting the growth (as would be possible with an anisotropic confinement geometry). Figure 1b-f presents representative SEMs of deposits generated with spatial confinement to the indicated circular diameter, d. With d = 1.6 μm, (Figure 1b) a lamellar morphology was observed and consisted of five vertically oriented features. These features are very similar to those observed for inorganic phototropic growth on unpatterned large scale (cm^2 area) substrates (Figure 1a). The outermost feature on each side of the confined area exhibited curvature imposed by the circular confinement pattern. Relative to d = 1.6 μm (Figure 1b), growth confined to d = 1.2 μm (Figure 1b) resulted in a similar morphology but consisted of two instead of three central features. Only a singular central feature was observed when d = 0.8 μm (Figure 1d), whereas for d = 0.4 μm (Figure 1e), a central feature was not produced and instead a vertically oriented central depression was bordered by a single feature on each side. When growth area was constrained to d = 0.2 μm, a single circular feature filled the growth region. These data demonstrate that inorganic phototropic growth, despite spatial confinement to wavelength scale dimensions, and the consequent lack of any ensemble phenomena that may occur in an unconstrained case, can generate morphological order and anisotropy, even with as few as two discrete structural features.

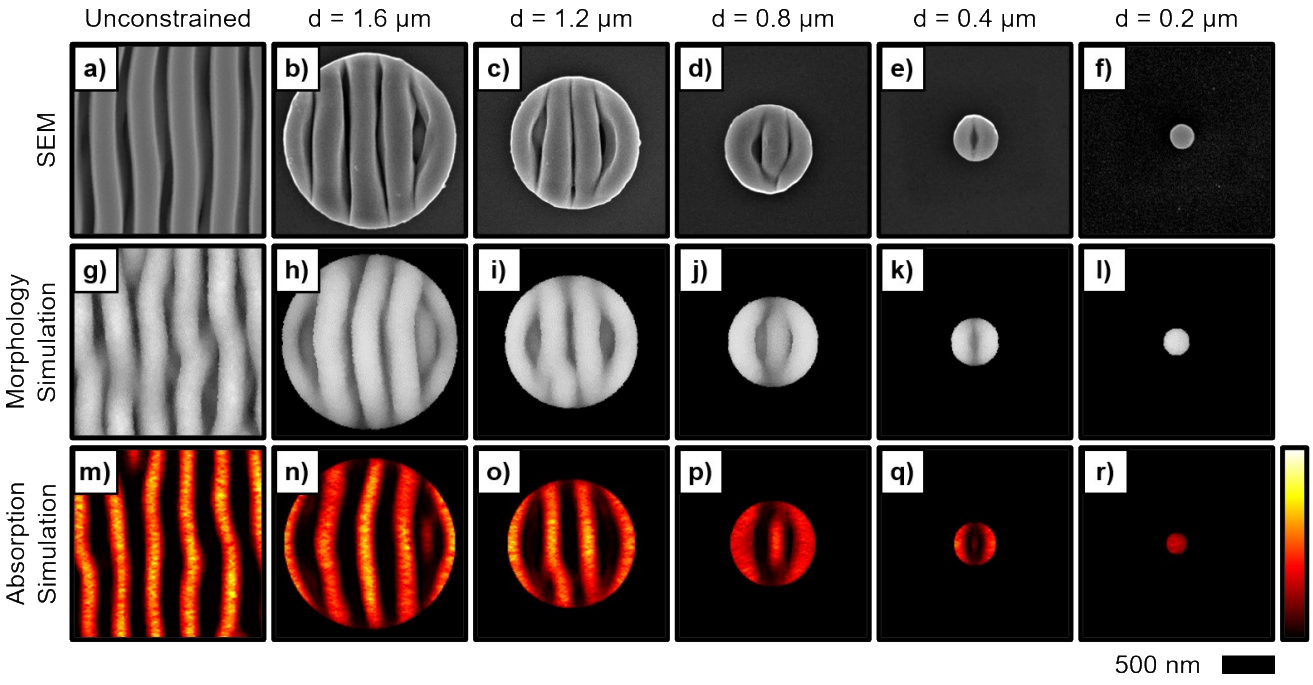

Figure 1. Representative SEMs of experimentally generated Se-Te deposits, grown from a solution of 0.0200 M SeO_2, 0.0100 M TeO_2, and 2.00 M H_2SO_4 using vertically polarized λ_{avg} = 934 nm illumination, without spatial constraint (a) and with areal constraint to the indicated circular diameter (b)-(f). Computer simulations of deposit morphologies generated via modeling of the growth (g)-(l) analogous to the empirical data in the above row. Light absorption profiles (m)-(r) corresponding to the simulated morphologies in the above row.

Computer simulations were performed to explore the principles that enable inorganic phototropic growth to direct morphological anisotropy and order at the wavelength scale. A two-step, iterative model with an optical basis was utilized to emulate the bottom-up growth process. First, an electromagnetic method was used to simulate illumination of the growth interface and calculate the magnitude of light absorbed at each point along the interface. Then, Se-Te mass was selectively added to the interface in a probabilistic fashion using a Monte Carlo method wherein the likelihood of mass addition at a certain location scaled with the local light absorption magnitude as determined in the previous step. Last these steps were successively iterated, with a new evaluation of the absorption in the evolved interface resulting from mass addition in the immediately previous iteration. This process has been shown to reproduce structural genesis and evolution of films generated by inorganic phototropic growth.[11] Empirical inputs were minimal and included estimates of the deposit complex refractive index and the electrolyte index. Figure 1g-l present simulated morphologies analogous to the experimental observations depicted in Figure 1a-f. Each simulated morphology is the result of a discrete, independent set of growth computations initialized from an isotropic substrate. In all cases, the simulated morphology was in remarkable accord with that observed experimentally. Such agreement between the experimental and computational data indicates that the structures observed experimentally are determined by optical processes as opposed to a chemical or crystallographic bias of the Se-Te material or any other physical processes, e.g. mass transport, during growth.[12-14]

Light absorption in the morphologies generated by the optically based, growth modeling was evaluated to assess the basis for structure determination. Figure 1m-r presents the spatial profiles of light absorption derived from the growth modeling that correspond to the simulations displayed in Figure 1g-l, respectively. For a spatially unconfined film (Figure 1m), the intensity in the absorption profile closely tracked the simulated film morphology (Figure 1g), with relatively high absorption along all the observed lamellar features and minimal absorption in the space between the features. When growth was confined spatially to d = 1.6 μm (Figure 1n), the highest absorption intensity was observed along the centermost feature, with some elevated absorption in the neighboring features near the vertical midpoints. A similar absorption profile was observed for growth when the spatial confinement was constrained to d = 1.2 μm (Figure 1o), with the largest intensity the middle of the central features. For d = 0.8 and 0.4 μm (Figure 1p and q), the absorption still tracked the principal growth features, but exhibited less contrast and was lower in magnitude than for d = 1.6 or 1.2 μm (Figure 1n and o). The lowest relative absorption, with minimal spatial variance in the circular area, was observed for d = 0.2 μm (Figure 1r). These data indicate a synergistic nanophotonic phenomenon in which the absorption in an individual feature is enhanced by the presence of additional adjacent features. Notably, an absorption profile that was very similar to that of the spatially unconfined growth (Figure 1m) was obtained with only four or five total parallel features (Figure 1o and n). These data indicate that the synergistic absorption in an individual feature is predominately determined by the contributions of the very nearest neighbors, suggesting that the self-organization observed during inorganic phototropic growth is primarily directed by short-range light-matter interactions within the optical near-field.

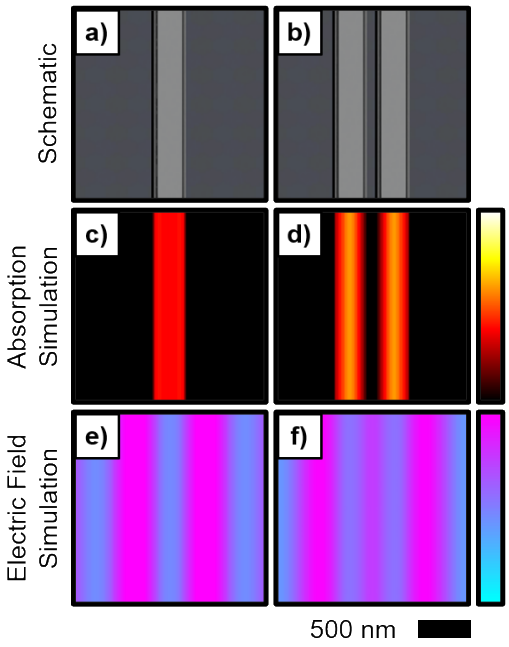

Figure 2. Schematic of simplified lamellar morphologies (a) and (b) and corresponding simulations of the light absorption (c) and (d) and time-average of the electric field magnitude (e) and (f).

Additional computational modeling was performed to further explore the optical interactions between neighboring deposit features and interrogate the length scale that is relevant and determinative of the emergent film growth evident in the experiments and simulations presented in Figure 1 for inorganic phototropic growth with circular spatial confinement. A simplified, idealized lamellar feature was designed with shape and dimensions characteristic of those observed experimentally. Structures with a single such feature, as well as one with two features separated by the feature pitch observed experimentally, were modeled and are presented schematically in Figure 2a and b. Spatial confinement, as was effected using a substrate patterned with circular well structures for the experimental as well as computational growth modeling investigations (Figure 1), was not utilized here. The structures were explicitly predefined rather than generated spontaneously, but experimental and simulated growth results demonstrate that analogous structures are generated spontaneously during inorganic phototropic film growth.

Stimulation was simulated with the same illumination utilized both experimentally and in the growth modeling, and the spatial absorption profiles were calculated and are presented in Figure 2c and d. Enhanced absorption was observed in the simulation that contained two features (Figure 2d) relative to that with the single feature (Figure 2c), consistent with the synergistic absorption phenomenon observed in the growth modeling data. Figure 2e presents a simulation of the spatial profile of the time-averaged electric field magnitudes corresponding to the absorption data in Figure 2c. An enhancement in the amplitude of the field was observed in the regions directly adjacent to the lamellar feature. Figure 2f presents a simulation analogous to that in Figure 2e, but for the case of two features (Figure 2b), showing a similar enhancement in the regions adjacent to the outer edges of the features. These data indicate that the features anisotropically scatter the incident illumination, effecting optical localization and concentration in the immediate vicinity of the feature of concern. Synergistic absorption thus occurs when a neighboring feature is present. Such scattering and absorption processes in the optical near-field consequently provide the basis for spontaneously ordered inorganic phototropic growth. These results indicate that inorganic phototropic growth can direct the morphological anisotropy and order at spatial scales comparable to the incident optical wavelength, in the absence of any emergent ensemble phenomena that may result at longer, extended length scales.

In summary, inorganic phototropic growth was performed over wavelength scale areas, and morphological anisotropy and order were observed in the deposits despite the limited length scale. The growth morphologies were simulated using a fully optically based model and were in close agreement with the experimental observations, indicating that the morphologies are primarily determined by optical phenomena. Light absorption in the simulated morphologies was analyzed and synergy was observed in which absorption in a single feature was enhanced by the presence of adjacent, neighboring features. The features scattered the incident illumination, enhancing the relative intensity in the directly adjacent regions. This scattering process thus feeds the absorption synergy, establishing the nanophotonic basis that promotes cooperative growth and demonstrating that extended ensemble phenomena are not necessary to direct structure and produce spontaneous organization in inorganic phototropic growth.

ASSOCIATED CONTENT

Supporting Information.

The Supporting Information is available free of charge on the ACS Publications website.

Details regarding experimental and modeling/simulation methods, additional computational data (PDF)

AUTHOR INFORMATION

Corresponding Author

*Email: nslewis@caltech.edu

Author Contributions

§These authors contributed equally (AIC and MCM)

Notes

The authors declare no competing financial interest.

ACKNOWLEDGMENT

This work was supported by the National Science Foundation, Directorate for Mathematical & Physical Sciences, Division of Materials Research under Award Number DMR 1905963. The authors gratefully acknowledge J. R. Thompson and W.-H. Cheng for insightful discussions, and R. Gerhart and N. Hart for assistance with photoelectrochemical cell fabrication. MCM and KRH acknowledge Graduate Research Fellowships from the National Science Foundation. MCM also acknowledges the Resnick Sustainability Institute at Caltech for fellowship support.

REFERENCES

(1) Christie, J. M.; Murphy, A. S. Shoot phototropism in higher plants: New light through old concepts. Am. J. Bot. 2013, 100, 35-46.

(2) Hutchings, M. J.; de Kroon, H. Foraging in Plants: the Role of Morphological Plasticity in Resource Acquisition. In Advances in Ecological Research; Begon, M., Fitter, A. H., Eds.; Academic Press: London, 1994; Vol. 25, pp 159-238.

(3) Slade, A. J.; Hutchings, M. J. The Effects of Light Intensity on Forgaing in the Clonal Herb Glechoma Hederacea. J. Ecol. 1987, 75, 639-650.

(4) Meier, M. C.; Cheng, W.-H.; Atwater, H. A.; Lewis, N. S.; Carim, A. I. Inorganic Phototropism in Electrodeposition of Se-Te. J. Am. Chem. Soc. 2019, 141, 18658-18661.

(5) Carim, A. I.; Batara, N. A.; Premkumar, A.; Atwater, H. A.; Lewis, N. S. Self-Optimizing Photoelectrochemical Growth of Nanopatterned Se-Te Films in Response to the Spectral Distribution of Incident Illumination. Nano Lett. 2015, 15, 7071-7076.

(6) Tan, C.; Qin, C.; Sadtler, B. Light-directed growth of metal and semiconductor nanostructures. J. Mater. Chem. C 2017, 5, 5628-5642.

(7) Carim, A. I.; Batara, N. A.; Premkumar, A.; May, R.; Atwater, H. A.; Lewis, N. S. Morphological Expression of the Coherence and Relative Phase of Optical Inputs to the Photoelectrodeposition of Nanopatterned Se-Te Films. Nano Lett. 2016, 16, 2963-2968.

(8) Carim, A. I.; Hamann, K. R.; Batara, N. A.; Thompson, J. R.; Atwater, H. A.; Lewis, N. S. Template-Free Synthesis of Periodic Three-Dimensional PbSe Nanostructures via Photoelectrodeposition. J. Am. Chem. Soc. 2018, 140, 6536-6539.

(9) Hamann, K. R.; Carim, A. I.; Meier, M. C.; Thompson, J. R.; Batara, N. A.; Yermolenko, I. S.; Atwater, H. A.; Lewis, N. S. Optically tunable mesoscale CdSe morphologies via inorganic phototropic growth. J. Mater. Chem. C 2020, 12412-12417.

(10) Carim, A. I.; Batara, N. A.; Premkumar, A.; Atwater, H. A.; Lewis, N. S. Polarization Control of Morphological Pattern Orientation During Light-Mediated Synthesis of Nanostructured Se-Te Films. ACS Nano 2016, 10, 102-111.

(11) Hamann, K. R.; Carim, A. I.; Meier, M. C.; Lewis, N. S. Path-Dependent Morphological Evolution of Se-Te Mesostructures Prepared by Inorganic Phototropic Growth. J. Am. Chem. Soc. 2020, 142, 19840-19843.

(12) Xiao, Z.-L.; Han, C. Y.; Kwok, W.-K.; Wang, H.-H.; Welp, U.; Wang, J.; Crabtree, G. W. Tuning the Architecture of Mesostructures by Electrodeposition. J. Am. Chem. Soc. 2004, 126, 2316-2317.

(13) Siegfried, M. J.; Choi, K.-S. Elucidating the Effect of Additives on the Growth and Stability of Cu2O Surfaces via Shape Transformation of Pre-Grown Crystals. J. Am. Chem. Soc. 2006, 128, 10356-10357.

(14) Liu, R.; Vertegel, A. A.; Bohannan, E. W.; Sorenson, T. A.; Switzer, J. A. Epitaxial Electrodeposition of Zinc Oxide Nanopillars on Single-Crystal Gold. Chem. Mater. 2001, 13, 508-512.


Absorption Synergy Directs Self-Organization